SCIENCE CHINA
Information Sciences

• MOOP •

May 2026, Vol. 69, Iss. 5, 154301:1–154301:3
https://doi.org/10.1007/s11432-025-4758-3

Experimental demonstration of forward distortion compensation based on amplitude-phase block modulation for nonlinear wireless communications

Min FAN[1], Cheng YI[2], Haiming WANG[1,2*], Wei XU[2,3], Bensheng YANG[4] & Xiaohu YOU[2,3]

[1]*State Key Laboratory of Millimeter Waves, Southeast University, Nanjing 211189, China*
[2]*Pervasive Communication Research Center, Purple Mountain Laboratories, Nanjing 211111, China*
[3]*National Mobile Communications Research Laboratory, Southeast University, Nanjing 211189, China*
[4]*School of Communications and Information Engineering, Nanjing University of Posts and Telecommunications, Nanjing 210023, China*

Received 20 August 2025/Revised 13 November 2025/Accepted 14 January 2026/Published online 16 March 2026

Citation Fan M, Yi C, Wang H M, et al. Experimental demonstration of forward distortion compensation based on amplitude-phase block modulation for nonlinear wireless communications. Sci China Inf Sci, 2026, 69(5): 154301, https://doi.org/10.1007/s11432-025-4758-3

High energy efficiency and broad coverage are essential requirements for 6G and beyond 6G (B6G) wireless communication systems, along with the deployment of millimeter wave (mmWave) and terahertz (THz) frequency bands [1, 2]. However, these evolutions have also exacerbated the nonlinear behavior of radio frequency (RF) hardware, particularly power amplifiers (PAs), which fundamentally limit system performance [3]. When PAs operate in their linear region with large power back-off, their power-added efficiency (PAE) is extremely low at mmWave and THz bands. In contrast, operating in the nonlinear region ensures a much higher PAE but introduces significant challenges, including severe out-of-band (OOB) emissions and in-band nonlinear distortion, which degrade both spectral efficiency and information transmission reliability. The nonlinear transform from the transmitted sequence $\mathbf{x} \in \mathbb{C}^{N\times 1}$ to the received sequence $\mathbf{y} \in \mathbb{C}^{N\times 1}$ is characterized by

$$\mathbf{y} = \mathcal{F}\{\mathbf{x}\} + \mathbf{z} = \mathbf{H}\mathbf{x} + \boldsymbol{\eta} + \mathbf{z}, \tag{1}$$

where $\mathcal{F}: \mathbb{C}^N \to \mathbb{C}^N$ denotes the nonlinear transform, $\mathbf{H} \in \mathbb{C}^{N\times N}$ denotes the linear channel matrix, $\mathbf{z}$ represents additive white Gaussian noise (AWGN), and $\boldsymbol{\eta}$ represents the signal-dependent nonlinear distortion introduced by the PA.

Existing solutions to cancel the nonlinear distortion term $\boldsymbol{\eta}$ can be broadly classified into model-based and data-driven approaches [3]. For example, Li et al. [4] proposed a nonlinear model that embeds an adaptive mismatch model into a well-matched model to compensate for the nonlinear distortion of the dynamic system configurations at the transmitters. He et al. [5] developed a unified time-domain representation for several PA models and proposed a corresponding nonlinear time-domain equalization method to apply the reverse process of $\mathcal{F}$ at the receivers. Based on Gaussian process regression and neural networks, two post-distorters were proposed to eliminate nonlinear distortion in the equalized signal at the receivers in [6]. Both approaches aim to invert the nonlinear mapping operation $\mathcal{F}\{\cdot\}$ to recover the transmitted sequence $\mathbf{x}$ from the distorted received sequence $\mathbf{y}$. Another line focuses on designing the transmitted sequence $\mathbf{x}$. A golden angle modulation-based orthogonal frequency division multiplexing (OFDM) system with an inherent low peak-to-average power ratio (PAPR) [7] and the corresponding generalized constellation mapping [8] were proposed to mitigate the PA nonlinearity $\boldsymbol{\eta}$ at the transmitter. Heuristically, amplitude-phase block modulation (APBM) schemes with specific constraints in $\mathbf{x}$ were proposed to compensate for nonlinear distortion without knowing the nonlinear model at receivers in single-carrier (SC) systems [9] and OFDM systems [10].

In this work, we experimentally demonstrate a forward distortion compensation (FDC) scheme based on APBM to collaboratively handle OOB emissions and in-band distortion in both SC and OFDM systems. The FDC architecture decouples in-band distortion and OOB radiation issues, as shown in Figure 1(a). At the transmitter, APBM is adopted to generate the waveform, and controlled nonlinear pre-processing is applied to suppress OOB emission at the cost of in-band distortions. At the receiver, an APBM constraint-based nonlinear distortion compensation is performed. The experimental results demonstrate that this approach yields remarkable PAEs and output powers in both SC and OFDM systems.

APBM-based waveform generation. Firstly, the transmitted bit stream is mapped to a constrained sequence $\mathbf{x}$ based on APBM, which enforces a constant power sum for adjacent symbol pairs. This property can be expressed as

$$\mathbf{A}\left(\mathbf{x} \odot \mathbf{x}^*\right) = P\mathbf{e}, \tag{2}$$

where $\mathbf{e}$ is an all-ones vector of dimension $\frac{N}{2} \times 1$, P is the constant power sum, $\odot$ denotes the Hadamard product, and superscript * denotes the conjugate operation. The sparse matrix $\mathbf{A} \in \mathbb{R}^{\frac{N}{2}\times N}$ is introduced to mathematically describe this pairwise relationship. It is constructed such that for each row index i, the only non-zero elements are $a_{i,2i-1} = a_{i,2i} = 1$. This constraint will be used for in-band distortion compensation at the receiver.

* Corresponding author (email: hmwang@seu.edu.cn)

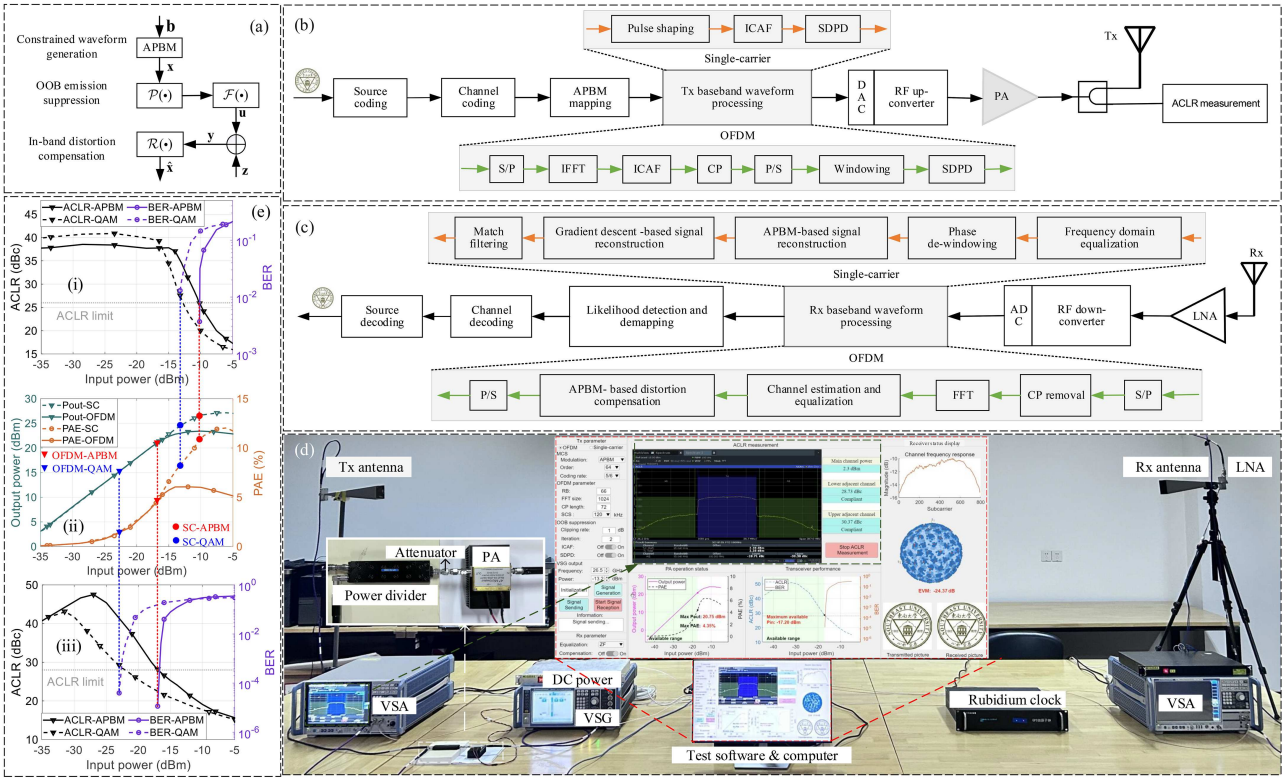

Figure 1 (Color online) (a) The APBM-based FDC scheme. (b) The nonlinear transmitter. (c) The nonlinear receiver. (d) The experimental platform for nonlinear wireless transmission. (e) Performance evaluation: (i) BER and ACLR of the SC system under test at 20 GHz; (ii) PAE and output power of the PA; (iii) BER and ACLR of the OFDM system under test at 26.5 GHz.

OOB emission suppression. Then, a nonlinear pre-processing $\mathcal{P}\{\cdot\}$ is performed before nonlinear power amplification, denoted by $\mathbf{u} = \mathcal{F}\{\mathcal{P}\{\mathbf{x}\}\}$. Unlike conventional methods that attempt to make $\mathbf{u}$ and $\mathbf{x}$ linear, $\mathcal{P}\{\cdot\}$ aims to suppress the OOB emission from the PA output. It consists of an iterative clipping and filtering (ICAF) with an extremely low clipping level and a static digital pre-distortion (SDPD) based on a rough PA modeling in this study, as shown in Figure 1(b). ICAF aggressively suppresses the signal PAPR, and SDPD avoids the additional computational overhead required for high-precision PA modeling. Although $\mathcal{P}\{\cdot\}$ suppresses OOB emissions, it introduces non-PA-induced in-band nonlinear distortion in the received sequence $\mathbf{y}$.

In-band nonlinear distortion compensation. Generally, the nonlinear distortion caused by the PA is sparse and related to power. The higher the power, the more severe the distortion. Sampling points with power less than a critical value P_c can be considered free from nonlinear distortion. ICAF exhibits characteristics similar to the PA, except that filtering also causes slight distortion to the low-power samples. Therefore, with a linear equalizer, the received sequence $\mathbf{y}$ can be expressed as

$$\mathbf{y} = \mathbf{x} + \mathcal{G}^{-1}\{\mathbf{m} \odot \boldsymbol{\eta} + \boldsymbol{\zeta}\} + \tilde{\mathbf{z}}, \tag{3}$$

where the operator $\mathcal{G}\{\cdot\}$ represents the pulse shaping filter for SC systems or the inverse discrete Fourier transform (IDFT) for OFDM systems, $\tilde{\mathbf{z}} = \mathbf{w}\mathbf{z}$ is the AWGN term after zero-forcing equalization, with $\mathbf{w}$ being the channel equalization matrix, and $\mathbf{m}$ is the sparse mask of the power-related distortion $\boldsymbol{\eta}$, defined as $\mathbf{m} = \mathcal{S}\{(\mathcal{G}\{\mathbf{x}\}) \odot (\mathcal{G}\{\mathbf{x}\})^* - P_c\mathbf{e}\}$. The step function $\mathcal{S}\{\cdot\}$ acts as a threshold detector, setting the mask elements $\mathbf{m}$ to 1 for samples whose power exceeds the critical value P_c, and to 0 otherwise. This formulation captures the physical characteristics of PA nonlinear distortion and the clipping process in ICAF, where distortion primarily affects high-power samples, while low-power samples are considered distortion-free. Furthermore, $\boldsymbol{\zeta}$ is the in-band distortion caused by filtering in ICAF, which can be easily estimated with a known ICAF configuration.

For the reliability of information transmission, receivers need to extract $\mathbf{x}$ from $\mathbf{y}$. Conventional QAM-based schemes require accurate nonlinear modeling of the distortions η and ζ in advance. The fundamental advantage of the APBM-based scheme lies in the constraint embedded within its signal structure. This constraint provides the receiver with powerful a priori information to combat nonlinear distortion. Based on the APBM constraint characteristics in (2), nonlinear signal reconstruction can be described as a constrained optimization problem, i.e.,

$$\begin{aligned} &\hat{\mathbf{x}} = \arg\min_{\mathbf{x},\boldsymbol{\eta},\boldsymbol{\zeta}} \|\mathbf{y} - \mathbf{x} - \mathcal{G}^{-1}\{\mathbf{m} \odot \boldsymbol{\eta} + \boldsymbol{\zeta}\}\|_2^2, \\ &\text{s.t. } \mathbf{A}(\mathbf{x} \odot \mathbf{x}^*) = P\mathbf{e}. \end{aligned} \tag{4}$$

The solution of (4) does not depend on accurate nonlinear modeling. The operator $\mathcal{G}\{\cdot\}$ determines the correlation of signal distortion between the time domain and the symbol domain, which motivates the use of different reconstruction algorithms for SC and OFDM systems. For an SC system, since the transmitted sequence is also in the time domain, the distortion characteristics of the signal are highly correlated with those of the transmitted sequence. The received sequence $\mathbf{y}$ can be directly reconstructed to meet the characteristics of sequence distortion and constraints. In this study, a constraint-based sequence crossover estimation and weighting in [9] is adopted to compensate for the distortion term η. Although the sequence after compensating for η is not identical to $\mathbf{x}$ due to the influence of ζ, it closely approximates $\mathbf{x}$. Hence, a gradient descent algorithm is adopted to compensate for ζ. However, for an OFDM system, the discrete Fourier transform at the

receiver extends the nonlinear distortion of each time-domain sampling point to all frequency-domain subcarriers. To address (4) for OFDM systems, an APBM-based alternating projection method is developed. Specifically, the estimated sequence $\hat{\mathbf{x}}$, with $\mathbf{y}$ as the initial value, is alternately projected onto a frequency-domain constraint set constructed by APBM and a time-domain constraint set determined by distortion characteristics, so that $\hat{\mathbf{x}}$ gradually approximates $\mathbf{x}$.

Experimental setup. To validate the APBM-based FDC scheme, we constructed a nonlinear wireless transmission experimental platform. This platform was designed to emulate the practical operation of both SC and OFDM systems under nonlinear amplification. The specific transceiver structures of FDC-based communication systems are shown in Figures 1(b) and (c). The SC system referred to the DVB standard with a 72-MHz channel occupied bandwidth. The upsampling rate and the rolloff factor of the root-raised cosine pulse shaping were 4 and 0.2, respectively. The OFDM system was configured with a 100-MHz channel bandwidth and a 120-kHz subcarrier spacing. The OOB emission and transmission reliability were observed under varying PA input powers, measured by the adjacent channel leakage ratio (ACLR) and bit error rate (BER), respectively. The maximum available output powers and PAEs of the tested PA were compared for different configurations under compliant ACLR and BER requirements. BER was generally required to be no more than 10^{-6}, while the ACLR requirements were related to the communication scenario. For the SC system, according to the satellite communications standard, the minimum ACLR was set at 26 dBc. For the OFDM system, the ACLR threshold is 28 dBc for the FR2 band, as specified by the 3GPP standard.

The experimental platform for nonlinear performance measurements was demonstrated in Figure 1(d). Mostly, it consisted of a vector signal generator (VSG), a commercial PA, a power divider, two vector signal analyzers (VSAs), and a computer with custom-designed software. The software controls and displays the transceiver status in real-time, including parameter configuration, ACLR test, constellation, PA operating status, and transceiver performance. The software generated the digital signal and output it to the VSG. The VSG converted the digital signal to an RF format with a preset frequency and power. The power divider splits the PA output into two paths: one to the transmitting antenna and the other, via an attenuator, to a VSA for ACLR monitoring. The receiving antenna and another VSA captured the transmitted RF signal and converted it to a digital format. The received digital signal was also processed by the software to observe the constellation and calculate the BER. The experiments were conducted at 20 GHz for the SC system and 26.5 GHz for the OFDM system.

Experimental results. Using a high-power commercial PA, the OOB emissions and transmission reliability of 64-order modulation schemes were evaluated. Detailed experimental results are presented in Figure 1(e). Subfigures (i) and (iii) illustrate ACLR and BER as functions of the PA input power. Subfigure (ii) displays the PAE and output power for the two configurations. The results compare the performance of the APBM-based scheme with the conventional QAM-based scheme.

Both transmission schemes were tested with SDPD at their respective optimal clipping rates, maximizing the input power that satisfies both ACLR and BER requirements. For 64-APBM, the optimal clipping rates were 0.5 dB for the SC system and 1 dB for the OFDM system. In contrast, the best performance of 64-QAM occurs when there is no clipping. As shown in the combined results of subfigures (i) and (ii), to meet the ACLR and BER requirements, the maximum available PA output power for the APBM-based SC system reaches 26.50 dBm. The corresponding value for the QAM-based SC system is 24.34 dBm, resulting in a relative improvement of 2.16 dB. Similarly, subfigures (ii) and (iii) jointly present the results for OFDM systems. For the APBM-based OFDM system, the maximum available PA output power is 20.67 dBm, while the value achieved by the QAM-based system is only 14.77 dBm, resulting in a relative gain of 5.90 dB. Furthermore, the PAEs of the two schemes in SC and OFDM systems were analyzed. For the SC system at 20 GHz, the optimal available PAE is 8.07% and 10.84% for the QAM-based and APBM-based schemes, respectively, showing a PAE improvement of 34.32%. The corresponding values for the OFDM system at 26.5 GHz are 1.18%, 4.27%, and 261.86%, respectively.

Conclusion. An APBM-based FDC scheme for nonlinear wireless communications has been experimentally validated, demonstrating superior performance in PA output power and PAE. The scheme has achieved significant PAE improvements for both the SC system and the OFDM system. These findings present a new pathway toward achieving sustainable and energy-efficient wireless communications.

Acknowledgements This work was supported in part by National Natural Science Foundation of China (Grant Nos. 62550015, 62501659) and Science Foundation of Jiangsu Province of China (Grant No. BG2025001).

Supporting information Videos and other supplemental documents. The supporting information is available online at info.scichina.com and link.springer.com. The supporting materials are published as submitted, without typesetting or editing. The responsibility for scientific accuracy and content remains entirely with the authors.

References

1 You X H, Wang C-X, Huang J, et al. Towards 6G wireless communication networks: vision, enabling technologies, and new paradigm shifts. Sci China Inf Sci, 2021, 64: 1–74
2 Wang C X, You X, Gao X, et al. On the road to 6G: visions, requirements, key technologies, and testbeds. IEEE Commun Surv Tutorials, 2023, 25: 905–974
3 Chafii M, Bariah L, Muhaidat S, et al. Twelve scientific challenges for 6G: rethinking the foundations of communications theory. IEEE Commun Surv Tutorials, 2023, 25: 868–904
4 Li W, Montoro G, Gilabert P L. Adaptive digital predistortion for user equipment power amplifiers under dynamic frequency, bandwidth, and VSWR variations. IEEE Trans Microwave Theor Techn, 2025, 73: 8175–8187
5 He J S, Huang S, Huang Y Z, et al. A unified power amplifier representation-based receiver equalization technique for nonlinear OFDM signal detection. IEEE Trans Commun, 2024, 72: 2260–2274
6 Salman M B, Guvensen G M. An efficient QAM detector via nonlinear post-distortion based on FDE bank under PA impairments. IEEE Trans Commun, 2021, 69: 7108–7120
7 Zhai X, Xiao L, Ding T, et al. Golden angle modulation aided differential OFDM-IM for LEO satellite communications. IEEE Commun Lett, 2024, 28: 1604–1608
8 Xiao L, Zhai X, Liu Y, et al. A unified bit-to-symbol mapping for generalized constellation modulation. China Commun, 2023, 20: 229–239
9 Fan M, Yi C, Xu W, et al. Amplitude-phase-time block modulation for resisting nonlinear amplification and its application for energy-efficient wireless communications. IEEE Trans Commun, 2025, 73: 2329–2343
10 Fan M, Yi C, Yang B, et al. Forward distortion compensation based on amplitude-phase-frequency block modulation for nonlinear OFDM wireless communications. IEEE Trans Commun, 2026, 74: 2907–2923